Carbon Status Constrains Light Acclimation in the Cyanobacterium *Synechococcus elongatus*[1]

Tyler D.B. MacKenzie, Robert A. Burns, and Douglas A. Campbell*

Department of Biology, University of New Brunswick, Fredericton, New Brunswick, Canada E3B 6E1 (T.D.B.M., R.A.B., D.A.C.); and Department of Biology and Coastal Wetlands Institute, Mount Allison University, Sackville, New Brunswick, Canada E4L 1G7 (D.A.C.)

Acclimation to one environmental factor may constrain acclimation to another. *Synechococcus elongatus* (sp. PCC7942), growing under continuous light in high inorganic carbon (Ci; approximately 4 mM) and low-Ci (approximately 0.02 mM) media, achieve similar photosynthetic and growth rates under continuous low or high light. During acclimation from low to high light, however, high-Ci cells exploit the light increase by accelerating their growth rate, while low-Ci cells maintain the prelight shift growth rate for many hours, despite increased photosynthesis under the higher light. Under increased light, high-Ci cells reorganize their photosynthetic apparatus by shrinking the PSII pool and increasing Rubisco pool size, thus decreasing the photosynthetic source-to-sink ratio. Low-Ci cells also decrease their reductant source-to-sink ratio to a similar level as the high-Ci cells, but do so only by increasing their Rubisco pool. Low-Ci cells thus invest more photosynthetic reductant into maintaining their larger photosystem pool and increasing their Rubisco pool at the expense of population growth than do high-Ci cells. In nature, light varies widely over minutes to hours and is ultimately limited by daylength. Photosynthetic acclimation in *S. elongatus* occurs in both high and low Ci, but low-Ci cells require more time to achieve acclimation. Cells that can tolerate low Ci do so at the expense of slower photosynthetic acclimation. Such differences in rates of acclimation relative to rates of change in environmental parameters are important for predicting community productivity under variable environments.

Photosynthetic organisms, including cyanobacteria, must balance the absorption of light energy and its use, primarily in the fixation of inorganic carbon (Ci; Fujita, 1997; Huner et al., 1998). In the light, photosynthetic organisms produce reductant from the photooxidation of water that must be rapidly consumed through reduction of molecules such as Ci, nitrogen, or O_2 to avoid overreduction of intermediate electron carrier pools and buildup of reactive byproducts (Sonoike et al., 2001; Kana et al., 2002). In the freshwater environments of *Synechococcus elongatus* (sp. PCC7942; Rippka and Herdman, 1992), however, the availability of the principal Ci reductant sink is highly variable (Cole et al., 1994). Cyanobacteria have evolved to cope with variations in light and Ci and have mechanisms to acclimate from one light regime or Ci condition to another.

In aquatic environments, light can vary widely within the lifetime of individual cells, on timescales of seconds to hours, from wave focusing, vertical mixing, cloud cover, and the daily cycle of the sun (Schubert et al., 1995). Thus, the rate of light acclimation and exploitation of changing light is an important factor in the survival and efficient photosynthesis of picoplanktonic cells such as *S. elongatus*. Fast and high-amplitude changes in light happen in the context of a variable environmental Ci concentration, influenced by water temperature, pH, exchange with the atmosphere, photosynthetic and respiratory activities of the plankton and benthos, and import from terrestrial sources (Cole et al., 1994). To maintain a high intracellular Ci concentration across variable environmental Ci concentrations, cyanobacteria can induce powerful carbon concentrating mechanisms (CCMs) to actively concentrate sparse environmental Ci into the cell using energy from photosynthesis, and then release internal Ci as CO_2 near Rubisco at concentrations sufficient for efficient assimilation into organic form by the Calvin cycle (Badger and Price, 2003).

S. elongatus has at least four Ci uptake systems (Badger and Price, 2003). Two are low-affinity constitutive CCMs that help mediate the transport of CO_2 and HCO_3^- when environmental Ci is relatively high. At least two others are higher affinity CO_2 and HCO_3^- transporters that are induced when environmental Ci is low, and use substantial additional energy above the requirements of carbon fixation to maintain an internal Ci concentration up to 1,000 times higher than external (Shibata et al., 2002; Badger and Price, 2003; Ogawa and Kaplan, 2003). There are constitutive and inducible CCMs for both CO_2 and HCO_3^- because the pH dependence and the slow equilibration of those forms

[1] This work was supported by the Natural Sciences and Engineering Research Council of Canada (NSERC) operating and equipment grants (to D.A.C.), NSERC postgraduate and University of New Brunswick Board of Governors scholarships (to T.D.B.M.), and the Mount Allison Coastal Wetlands Institute funded by the Canada Foundation for Innovation and Atlantic Canada Opportunities Agency.

* Corresponding author; e-mail dcampbell@mta.ca; fax 506–364–2505.

Article, publication date, and citation information can be found at www.plantphysiol.org/cgi/doi/10.1104/pp.104.047936.

can alter the proportional availability of CO_2 and HCO_3^- in the Ci pool (Shibata et al., 2002; Raven, 2003). *S. elongatus* (Rodríguez-Buey and Orús, 2001) cells grown bubbled with air (approximately 370 μmol CO_2 mol^{-1}) induce a high-affinity CCM with a K_m of 14 μmol Ci, which maintained growth rates nearly as high as *S. elongatus* cells grown bubbled with 50,000 μmol CO_2 mol^{-1} air, which had a K_m of 281 μmol mol Ci. Thus, synthesis and maintenance of the CCM requires significant investments and rearrangements for cells growing in low-Ci environments, but nonetheless, under steady light and nutrient supplies, low-Ci cells can maintain photosynthesis and growth at levels comparable to high-Ci cells without the same energetic and metabolic constraints of the induced CCM.

We hypothesized that the induced CCMs in low-Ci cells would, however, constrain the rate and amplitude of light acclimation. Light and Ci are major environmental factors that interactively constrain the organization of the photosynthetic apparatus. In cyanobacteria, abundant complexes, including phycobilisome antennae, two photosystems, intersystem electron transport components, and terminal electron sinks, absorb and convert light energy into reductant (electrons) and chemical energy (ATP) for the biosynthesis of cell components and the maintenance of cell functions, including the self-same photosynthetic apparatus. The organization of the photosynthetic apparatus is in a dynamic balance (Kana et al., 1997) that is driven by the environment, in part through the redox status of the intersystem electron transport components (Fujita, 1997; Huner et al., 1998). Environmental signals, such as light, temperature, and availability of electron sinks, are integrated as excitation pressure in the electron transport system (Huner et al., 1995), which is controlled through photosystem antenna size (Escoubas et al., 1995; Durnford and Falkowski, 1997), stoichiometry of PSII and PSI (Fujita et al., 1987; Smith and Melis, 1988), Rubisco content (Li and Tabita, 1994; Kaplan et al., 2001), and perhaps CCM induction (Woodger et al., 2003; McGinn et al., 2004). Changes in external Ci also result in major reorganization of the photosynthetic system as part of the induction of the CCM (Kaplan et al., 2001), in which the additional energy required to power the CCMs is derived through cyclic (Herbert et al., 1995; Ogawa and Kaplan, 2003) or pseudocyclic electron transport back to O_2 (Li and Canvin, 1997; Allen, 2003). The pressures on photosystem organization caused by the requirements of induced CCMs interact with signals for balancing excitation pressure, resulting in cells metabolically distinct from high-Ci acclimated cells, with presumably altered acclimation mechanisms to accommodate the two environmental imperatives.

In this study, we quantified the organization and performance of the photosynthetic apparatus in high- and low-Ci cells, and how that organization and performance changed during and after acclimation to a steep increase in light. We measured overall photosynthetic function before and after the light increase by light response curves of O_2 evolution (net reductant production), PSII function using fluorescence signals, and PSI function using specific absorbance change signals (Fig. 1). These complementary methods are noninvasive and detect the activities of the photosystems in situ (Krause and Weiss, 1991; Henley, 1993; Klughammer and Schreiber, 1994). Here, we report on the interactive and pervasive effect of Ci status on light acclimation in *S. elongatus* in terms of photosystem organization and excitation pressure balance, the rates and fates of photosynthetic reductant flow, and ultimately the cellular capacities to exploit increased light to sustain population growth.

RESULTS

High Carbon Status Allowed Rapid Exploitation of Increased Light

Under steady illumination of 50 μmol photons m^{-2} s^{-1}, *S. elongatus* cultures grew at nearly identical rates of about 2 doublings per day, under markedly different high- and low-Ci levels (Fig. 2). Similarly, high- and low-Ci cultures under long-term, continuous 500-μmol photons m^{-2} s^{-1} both grew at about 2.8 doublings per day. To minimize complications from self-shading as cell numbers increased in the shifted cultures, separate cultures grown under continuous high-light (HL) illumination to about 1.5 μg chlorophyll (Chl) *a* mL^{-1} were used to determine the growth rates of cultures fully acclimated to HL.

Under continuous illumination, the induced CCM activity could produce a high enough intracellular Ci to allow the low-Ci cells to maintain a growth rate similar to the high-Ci cells, as found previously (Rodríguez-Buey and Orús, 2001), over a large part of the tolerable light range for this organism. During acclimation to HL, however, the high-Ci cells quickly exploited the higher light and increased their growth rate to nearly double their preshift values within 4 h of the shift to HL, after which their growth rate began to decline again toward the continuous HL value (Fig. 2). By contrast, low-Ci cells could not quickly exploit the light increase, and instead initially suffered a decline in growth rate after the shift to HL, which only recovered to values similar to preshift growth rates after 4 h of growth under HL, with subsequent slow increase to the continuous HL value.

Net Photosynthetic Reductant Production after HL Shift

Both the high- and low-Ci cells had a similar large capacity for net photosynthetic reductant production, measured as net O_2 evolution, before and after the shift to HL, which increased only somewhat after growth under HL for 6 h (Fig. 3). The greatest change in achieved O_2 evolution occurred because of the shift

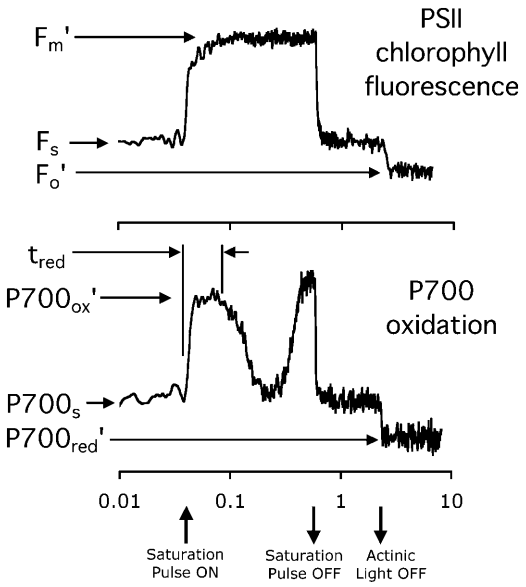

Figure 1. Sample response profiles of Chl fluorescence and P700 oxidation during a white-light ($\lambda < 695$ nm) saturation pulse of about 9,000 μmol photons m^{-2} s^{-1} for 0.5 s. The Chl fluorescence parameters F_m' (maximum fluorescence), F_s (steady-state fluorescence), and F_o' (minimum fluorescence) and the P700 oxidation parameters $P700_{ox}$ (fully oxidized), $P700_s$ (steady-state oxidation), $P700_{red}$ (fully reduced P700), and t_{red} (the time for reductant to travel through the intersystem electron transport chain to PSI) are indicated on the respective traces and are described in the text. Note the time axis is logarithmic to better show the details of the rapid induction kinetics in the context of the other fluorescence and oxidation parameters.

from the light-limited range of the light response curve to the light-saturated range immediately upon exposure to HL, causing an approximate doubling of O_2 evolution in both the high- and low-Ci cells. The light-saturated O_2 evolution rose further by 25% in both high- and low-Ci cells after 6 h of acclimation to HL. The light response curves in both high- and low-Ci cells showed slight drops in their initial slope (α) 6 h after the shift to HL compared with before the light shift, indicating a slight drop in the light-absorption capacity of the cells, which is consistent with the small concurrent drops observed in pigments per cell and functional absorption cross-sections of the photosystems (Table I). Our O_2 evolution measurements were made under incandescent light while the cells grew under fluorescent light. The incandescent source used for the O_2 evolution measurements provides relatively more red photosynthetically utilized radiation (PUR) per measured light than the fluorescent light under which the cultures grew, which may have caused an overestimate of quantum yield under the incandescent measuring light compared to the fluorescent growth light (Markager and Vincent, 2001). Despite the differences in spectra of the light sources, the optimal light intensity (E_k) for O_2 evolution in both cell types before the light shift was approximately 50 μmol photons m^{-2} s^{-1}, the same as the light level under which the cells were growing. Six hours after the shift to HL, E_k rose to 147 μmol photons m^{-2} s^{-1} in high-Ci cells and to 81 μmol photons m^{-2} s^{-1} in low-Ci cells by 6 h after the HL shift (Table I).

Changes in Photosystem Excitation Balance after HL Shift

The balance of the redox states of PSII and PSI were remarkably different between high- and low-Ci cells in response to the HL shift (Fig. 4). In both high- and low-Ci cells, by 6 h after the HL shift the proportion of open PSII centers at 500 μmol m^{-2} s^{-1} nearly doubled (Fig. 4A). There was also near doubling of the proportion of open PSI centers in the high-Ci cells but not in the low-Ci cells (Fig. 4B). The pressure was generally balanced between PSII and PSI in both high- and low-Ci cells under low light (LL) before the light shift (Fig. 5). Excitation pressure under HL in the high-Ci cells transiently fell disproportionately on PSI immediately after the light shift (low ratio of open PSI to open PSII) but returned to balance between PSII and PSI by 6 h after the light shift. In low-Ci cells, however, this excitation imbalance toward PSI after the light shift was larger and sustained. Even those low-Ci cells grown in continuous HL maintained an excitation pressure imbalance toward PSI.

Stoichiometric Changes in the Photosynthetic Apparatus

Even though high- and low-Ci cells had similar growth rates under the same illumination before the light shift, the stoichiometric organization of the photosynthetic apparatus in the two cell types was remarkably different (Table I). The high-Ci cells before the HL shift had a lower PSI-to-PSII ratio and a higher PSII functional absorption cross-section compared to low-Ci cells. The product of photosystem pool size and functional absorption cross-section is a measure of the

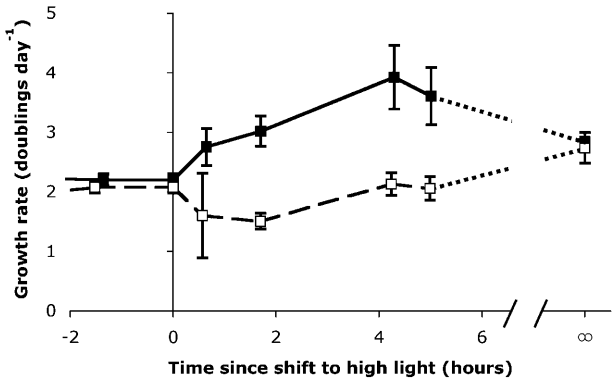

Figure 2. Growth rates of high-Ci (black symbols, solid line) and low-Ci (white symbols, dashed line) cultures of *S. elongatus* measured at various times (*x* axis) relative to the shift from LL (50 μmol m^{-2} s^{-1}; time <0) to HL (500 μmol m^{-2} s^{-1}; time >0). The growth rates of separate cultures grown continuously under HL are shown at time = ∞, and connected to the light-shifted cells by dotted lines (values are means, $n = 6 \pm$ SEM).

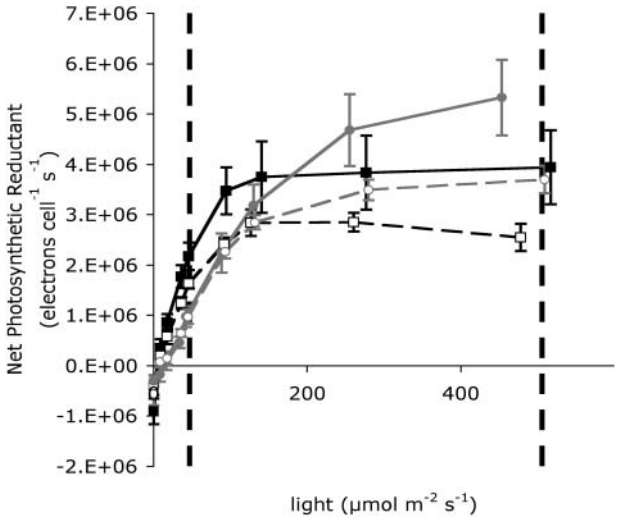

Figure 3. Light response curves of net photosynthetic reductant production determined from O_2 evolution measurements. High-Ci (black symbols, solid line) and low-Ci (white symbols, dashed line) light response curves are shown for cells grown at LL (50 μmol m^{-2} s^{-1}; black squares) and 6 h after shifting to HL (500 μmol m^{-2} s^{-1}; gray circles). Values are means, $n = 6 \pm$ SEM. Vertical dashed lines show LL and HL levels.

functional absorption capacity allocated to the photosystem pool. The ratio of functional absorption capacity of PSII was approximately equal between PSII and PSI in the high-Ci cells, while the functional absorption capacity of PSI was nearly twice that of PSII in the low-Ci cells, suggesting a higher priority on PSI activity likely for cyclic electron flow to power the CCMs. After the shift to HL, both PSII and PSI functional absorption capacities dropped by about 60% in the high-Ci cells. In low-Ci cells, however, PSI functional absorption capacity dropped disproportionately to also bring the capacities of PSII and PSI to approximate equality after the light shift. Despite the different photosystem organization of the high- and low-Ci cells, the excitation pressure on turnover rate of PSII were approximately the same in high- and low-Ci cells under LL before the light shift, and allowed a similar increase in PSII openness after the shift to HL.

Rubisco rose substantially in both high- and low-Ci cells (Fig. 6) after the light shift. The ratio of PSII absorption capacity to Rubisco concentration is an index of the allocations to photosynthetic reductant source versus sink in the cell because the source of reductant is PSII, and the primary sink for reductant is carbon fixation in the Rubisco-mediated Calvin cycle. The source-to-sink allocation ratio was larger in high-Ci cells than in low-Ci cells before the light shift, and they both dropped considerably after the light shift to converge at approximately the same value after 6 h in HL (Table I).

The drop in source-to-sink allocation in high-Ci cells occurred primarily via a sharp decline in the functional PSII content of the cells, and to a lesser extent the absorption cross-section (σ_{II}) of PSII. Photosynthetic rate was maintained in the smaller functional PSII pool by increasing PSII turnover rate (τ^{-1}) and the speed of electron transfer from PSII to PSI, leading to the observed increase in E_k. By contrast, low-Ci cells maintained their functional PSII pool and decreased their source-to-sink ratio only by increasing their Rubisco pool. These cells did not substantially increase the PSII turnover rate, nor did they decrease the time required for reductant to travel from PSII to PSI (t_{red}), as compared to high-Ci cells.

Our estimation of cell numbers based upon A_{750} may be underestimated after 6 h of growth in HL, as after extended growth at HL, cells per A_{750} eventually increase slightly. This may have led to a slight

Table I. *Pigmentation, photosystem stoichiometry, and flux changes resulting from the HL shift in high- and low-Ci cells*

All pigment, photosystem and protein values are expressed in molecules or complexes cell^{-1}. Values are means with $n = 6$, $\pm$ SEM.

	High-Ci Preshift	High-Ci Postshift	Low-Ci Preshift	Low-Ci Postshift
Phycocyanin ($\times 10^6$ molecules cell^{-1})	13.1 ± 1.1	10.0 ± 0.5	6.9 ± 0.4	5.7 ± 0.4
Chl *a* ($\times 10^6$ molecules cell^{-1})	17.2 ± 0.8	12.3 ± 0.7	12.6 ± 0.3	11.3 ± 0.3
Phycocyanin/Chl *a*	0.76 ± 0.04	0.82 ± 0.04	0.52 ± 0.03	0.50 ± 0.03
σ_{PSII} (nm^2)	1.15 ± 0.04	1.01 ± 0.08	1.06 ± 0.05	0.85 ± 0.09
σ_{PSI} (nm^2)	0.42 ± 0.13	0.29 ± 0.05	0.45 ± 0.11	0.34 ± 0.05
PSII ($\times 10^4$ complexes cell^{-1})	4.6 ± 0.4	2.2 ± 0.3	2.7 ± 0.2	2.8 ± 0.3
PSI ($\times 10^4$ complexes cell^{-1})	16.2 ± 0.9	12 ± 0.6	12.9 ± 0.4	10.8 ± 0.4
PSI-to-PSII ratio	3.7 ± 0.4	5.7 ± 0.7	4.9 ± 0.4	4.2 ± 0.5
PSII absorption capacity ($\times 10^4$ nm^2 cell^{-1})	5.3 ± 0.7	1.7 ± 0.4	2.8 ± 0.2	2.3 ± 0.2
PSI absorption capacity ($\times 10^4$ nm^2 cell^{-1})	4.5 ± 1.6	1.8 ± 0.6	4.3 ± 1.2	2.5 ± 0.3
RbcL ($\times 10^4$ molecules cell^{-1})	27 ± 9	83 ± 19	28 ± 11	83 ± 19
Excitation pressure $PSII_{500}$	0.68 ± 0.01	0.53 ± 0.03	0.64 ± 0.03	0.48 ± 0.01
τ^{-1} (s^{-1})	143 ± 17	341 ± 41	127 ± 7	162 ± 20
t_{red} (ms)	33.7 ± 3.6	25.2 ± 2.3	39.0 ± 6.7	55.6 ± 2.6
PSII capacity/Rubisco (nm^2 active site^{-1})	0.211 ± 0.065	0.034 ± 0.008	0.133 ± 0.062	0.037 ± 0.014
E_k (μmol m^{-2} s^{-1})	52.4 ± 7.3	146.9 ± 24.0	50.0 ± 1.6	80.6 ± 7.3

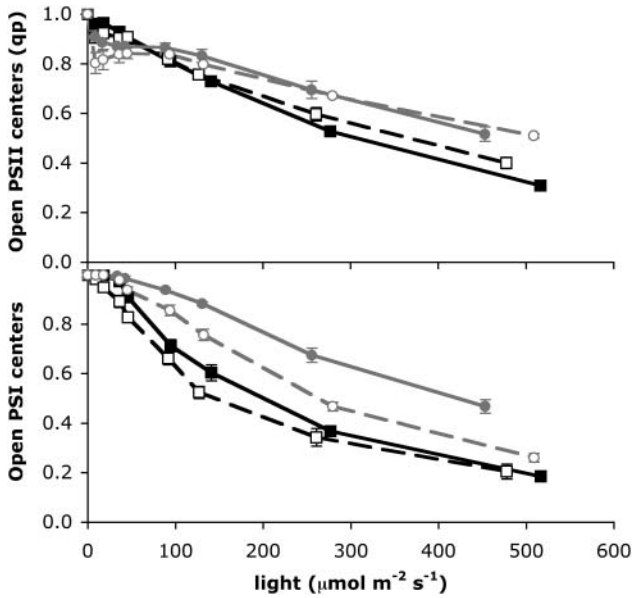

Figure 4. Openness or fraction of photosystems available for photosynthesis in PSII and PSI. High-Ci (black symbols, solid line) and low-Ci (white symbols, dashed line) light response curves are shown for cells grown at LL (50 μmol m^{-2} s^{-1}; black squares) and 6 h after shifting to HL (500 μmol m^{-2} s^{-1}; gray circles). Values are means, $n = 6 \pm$ SEM.

overestimate in the per-cell pool sizes of pigments, photosystems, and Rubisco in the postlight shift samples reported in Table I; however, this potential overestimation would have no effect on photosystem stoichiometries, source-to-sink relationships, or other parameters not standardized to cell number.

Growth Yield of Photosynthetic Reductant

High- and low-Ci cells showed similar increases in O_2 evolution but different growth rates after the HL shift, indicating a disparity in the photosynthetic reductant required for growth of the two cell types. High-Ci cells maintained a more balanced growth yield of photosynthetic reductant than did the low-Ci cells (Fig. 7). Before the light shift, all of the reductant could be accounted for by cellular growth in the high-Ci cells. Our growth yield of photosynthetic reductant was potentially overestimated, as literature values of the elemental composition of different strains of *Synechococcus* vary (Bertilsson et al., 2003; Heldal et al., 2003), not all nitrogen is assimilated via the reductive amination pathway, with its requirement for additional reductant, and not all sulfur in the cells was in the S^{2-} oxidation state (thiol sulfur). This calculation relating the requirements of the cells for balanced growth with the reductant produced by photosynthesis is complicated by the different spectra of the growth and measuring lights, especially in the limiting preshift light. The red-rich light of the incandescent source, having relatively high PUR per measured light, would likely overestimate quantum yield and, thus, the production of reductant in limiting light compared to the same light level in the growing cultures under fluorescent light. This effect would be more pronounced in high-Ci cells because of their relatively high phycocyanin content compared to low-Ci cells, and would be most effective in the limiting light preshift conditions than after the shift to HL. Under 500 μmol photons m^{-2} s^{-1}, the slight differences between the light sources in PUR per measured light would be physiologically irrelevant because at such HL levels, rates of turnover and consumption of reductant and energy generated by photosynthesis supersede quantum yield as a photosynthesis-limiting factor (Markager and Vincent, 2001).

Regardless of the factors contributing to error in the reductant requirements of cell growth, it is clear that the low-Ci cells produced more reductant relative to their requirement for balanced growth than did the high-Ci cells. The growth yield of reductant in LL, low-Ci cells was 25% less than the high-Ci cells, with about 87% of the reductant required for growth. After the shift to HL, the growth yield of reductant dropped in both high- and low-Ci cells, as photosynthesis shifted up the light response curve and increased more than did growth. In the high-Ci cells, the drop was relatively small and returned to preshift balance after 6 h under HL, while in the low-Ci cells the drop was more pronounced and sustained. These depressions of the growth yield of photosynthetic reductant may indicate an imbalanced investment of electrons between growing the cell population and the macromolecular pools contained in those cells, or a dumping of excess electrons into the reduction of carbon for extracellularly excreted organic compounds (Otero and Vincenzini, 2004).

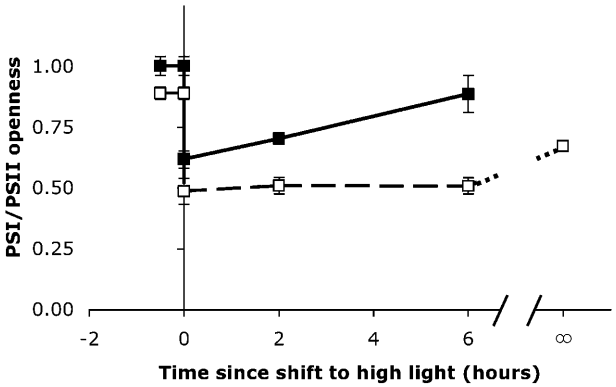

Figure 5. Balance of photosystem openness in high-Ci (black symbols, solid line) and low-Ci (white symbols, dashed line) cells measured at various times (x axis) relative to the shift from LL (50 μmol m^{-2} s^{-1}; time <0) to HL (μmol m^{-2} s^{-1}; time >0). The growth rates of separate cultures grown under HL continuously are shown at time $= \infty$, and connected to the light-shifted cells by the dotted line (values are means, $n = 6 \pm$ SEM). A continuous light value for high-Ci cells could not be calculated because the weak P700 absorbance values did not allow accurate PSI openness calculations. The error bars on some samples are smaller than the symbol size and thus are not visible.

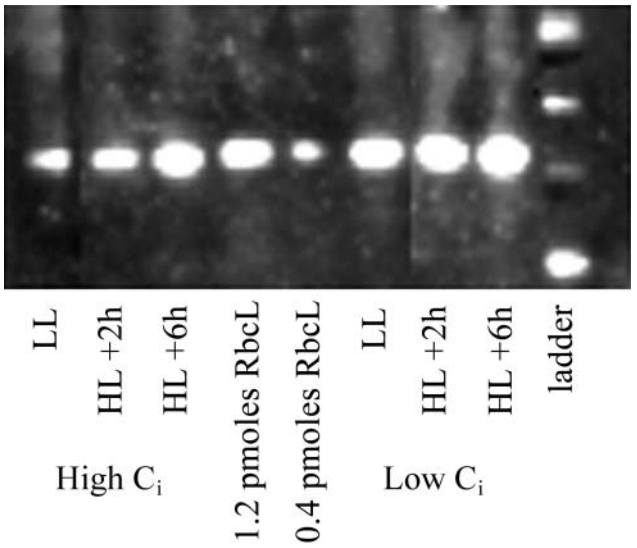

Figure 6. Representative chemiluminescent blot showing the content of RbcL detected by specific global anti-RbcL antibody in high- and low-Ci before and after the HL shift. At least two lanes per gel were loaded with a Rubisco quantitation standard (AgriSera). Quantitation of RbcL from similar replicate blots is presented in Table I.

DISCUSSION

The induction of a high-affinity CCM allows *S. elongatus*, under continuous illumination and mineral nutrient repletion, to maintain photosynthesis and growth at remarkably similar rates across a wide range of external Ci concentrations. These similar rates were maintained in part through compensatory changes of photosystem stoichiometry in cells grown in high- and low-Ci, a phenomenon originally described in *Anacystis nidulans* (currently named *S. elongatus*) as CO_2 control over their pigmentation (Eley, 1980). In the prelight shift cultures grown for many generations at 50 μmol m^{-2} s^{-1}, the high- and low-Ci cells also achieved balanced excitation of their photosystems, despite their differences in photosystem stoichiometry and Ci status. The photosystem stoichiometry difference between high- and low-Ci cells and restriction of the carbon sink in the low-Ci cells, however, caused different rates of acclimation to a sudden increase in light. High-Ci cells quickly exploited the higher light and were able to substantially increase their growth rate. Low-Ci cells, by contrast, which had a strong ability to concentrate the otherwise limiting low external Ci concentration, did so at the expense of rapid acclimation and did not increase their growth rate after the HL shift. After the shift to HL, the growth rate of the low-Ci cells remained at or below the preshift levels for many hours, despite a rapid and large increase in reductant produced; thus, the growth yield of photosynthetic reductant dropped after the shift to HL. The remaining reductant production in the initial hours following the light shift was likely invested in the rapid accumulation of an increased Rubisco pool while simultaneously increasing PSII synthesis to maintain a steady PSII pool in the face of more rapid PSII photoinactivation under HL, as well as in presumed increases of CCM capacity to better coordinate Ci accumulation with the increased photosynthetic rate.

Responses of Photosynthesis and the Photosynthetic Apparatus to the HL Shift

The light response curves of net photosynthetic electron production, measured as O_2 evolution, remained remarkably similar before and after the shift to HL, with the increase in electron flux primarily a result of the change in light with only limited changes in the light response of O_2 evolution. The stability of the light response curves was despite great changes in the photosynthetic apparatus, particularly in the PSII pool, and may help maintain biosynthesis and growth rate in the face of a sudden and potentially photoinhibitory 10-fold increase in light. In both the high- and low-Ci cells, there was a substantial initial decline in PSII pool size that did not affect the saturated rate of photosynthesis under the new HL condition. Several authors have demonstrated a similar large capacity of PSII in excess of the rate of net reductant produced, as O_2 evolved or CO_2 fixed (Sukenik et al., 1987; Behrenfeld et al., 1998; Kana et al., 2002). This excess capacity of electron transport could allow flexibility for coping with fluctuating light environments and transiently excess light (Behrenfeld et al., 1998), or act as a relief valve during acclimation to new light regimes (Campbell et al., 1998; Allen, 2003), especially in low-Ci samples with their restricted carbon reductant sink (Li and Canvin, 1997; Ort and Baker, 2002). The importance of a large capacity for PSII-generated reductant flowing through linear electron transport back to O_2 to power the CCMs of low-Ci cells has been demonstrated in cyanobacteria (Li and Canvin, 1997).

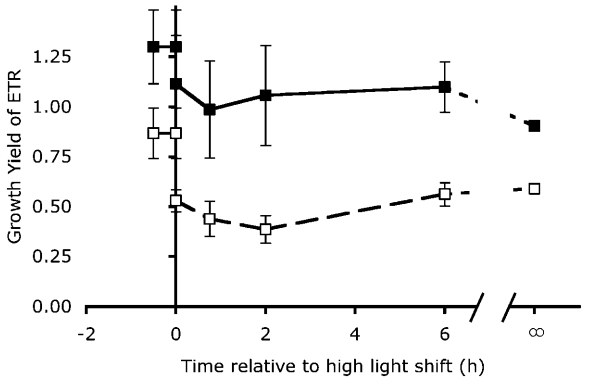

Figure 7. Growth yield of photosynthetic reductant, calculated as the ratio of the reductant generated from O_2 evolution (electron transport rate [ETR]) to the reductant required for producing cells at the observed growth rates (Eq. 9, "Materials and Methods"), in high-Ci (black symbols, solid line) and low-Ci (white symbols, dashed line) cells measured at various times relative to the shift from LL to HL. The values of separate cultures grown under HL continuously are shown at time = ∞ and connected to the light-shifted cells by dotted lines (values are means, $n = 6 \pm$ SEM).

Such a stability of O_2 evolution light response curves can be seen in several light acclimation studies in cyanobacteria (e.g. Vierling and Alberte, 1980) and algae (e.g. Schubert et al. 1995), but it is often confused because O_2 evolution is usually expressed per Chl and not per cell. This confusion was addressed by Vierling and Alberte (1980), who measured a doubling in O_2 evolution per Chl during light acclimation of *A. nidulans*, while O_2 evolution per cell remained within 2%, simply because of changes in cellular pigment content. This suggests that the cells maintain cell-limited near-optimum electron transport capacity over a range of light intensities.

Light Acclimation of Photosystem Stoichiometry

Several studies, including ours, have shown that changes in photosystem stoichiometry, and less so in the pigmentation of the photosystems, are an important component of light acclimation in cyanobacteria (Manodori and Melis, 1984; Murakami et al., 1997) and algae and plants (Melis and Brown, 1980). Changes in the pools of photosynthetic complexes occur to balance the absorption of light energy and its partitioning into the production of reductant and ATP, and to minimize the generation of dangerous reactive by-products of that energy (Fujita, 1997; Anderson et al., 1998; Allen, 2003). The PSI-to-PSII ratio varies from 0.3 in developing pea leaves (Melis and Brown, 1980) to at least 5 in cyanobacteria, with the highest ratios in cyanobacteria grown in low Ci and LL (Manodori and Melis, 1984; Müller et al., 1993). Cyanobacteria likely have a wider range of photosystem stoichiometries than higher plants because of the greater flexibility of their noncompartmentalized photosynthetic electron transport, which interacts with the respiratory electron transport system, and for cyclic electron transport to power transport processes like CCM activity (Manodori and Melis, 1984; Ogawa and Kaplan, 2003).Cyanobacteria acclimated to HL typically have lower PSI-to-PSII ratios than those acclimated to LL (Miskiewicz et al., 2002; Muramatsu and Hihara, 2003), in a process largely mediated by modulating the synthesis rate of PSI (Fujita, 1997). Upon exposing a mutant of *Synechocystis* PCC6803 unable to modify photosystem stoichiometry to HL, photosynthesis and growth rate were initially increased over the wild type, but the mutants later succumbed to photoinhibition and death because of the imbalanced stoichiometry (Sonoike et al., 2001). Changes of PSI-to-PSII and PSII-to-Rubisco stoichiometry have been observed in cyanobacteria acclimating to different light intensities (Murakami and Fujita, 1991a), spectral qualities (Fujita, 1997), and availabilities of CO_2 (Manodori and Melis, 1984; Müller et al., 1993).

In this study, we observed a transient but large increase in the functional PSI-to-PSII ratio in high-Ci cells shifted to HL, largely through a drop in the functional PSII pool size. This drop in functional PSII allowed cells to maintain efficient reductant flow into carbon fixation while it relieved excess pressure on the electron transport system and allowed a rapid, but ultimately transient, growth burst. This transient compensatory pattern in the PSII pool has been observed in natural phytoplankton assemblages periodically mixed into HL surface waters, and in cultured diatoms and green algae transiently exposed to HL (Vasilikiotis and Melis, 1994; Behrenfeld et al., 1998; Kana et al., 2002). The drop in PSII, caused by photodegradation (Clarke et al., 1992; Öquist et al., 1992) or rapid cell division diluting the PSII pool (Webb and Melis, 1995), is an important resource-efficient acclimatory response. We estimated a drop of PSII per cell of 56% after 2 h under HL in the high-Ci cells, nearly 3 times faster than the division rate of the cells. This increase in the net rate of photodegradation of PSII (Clarke et al., 1992) helped shrink the PSII pool through a transient slowing or cessation of investment into PSII synthesis as part of a mechanism to decrease the source-to-sink ratio of the cells. By contrast, the low-Ci cells initially maintained a smaller PSII pool under LL, which declined slightly upon the shift to increased light but rapidly recovered back to preshift levels by 6 h after the shift, showing increased investment to maintain PSII pools across the light shift in the face of increased photodegradation. Low-Ci cells also supported a larger increase in the Rubisco pool to decrease their source-to-sink ratio. These distinct changes to the photosynthetic apparatus in the high- and low-Ci cells, as well as a potential need to increase the capacity of the CCMs in the low-Ci cells shifted to higher light, can largely explain the differences in the growth yield of reductant in the two cell types.

Changes in Excitation Balance and the Fate of Photosynthetic Electron Transport

The large change in photosystem stoichiometry in the high-Ci cells in response to the light shift allowed a rapid and balanced relief of excitation pressure on both PSII and PSI. This relief of excitation, and progressive balancing of the redox state of the two photosystems after the shift to HL, shows that the changing photosystem stoichiometry and source-to-sink ratios worked to increase electron transport while minimizing dangerous overenergization of the photosynthetic system. Presumably, the overpressured and imbalanced excitation of the two photosystems upon HL exposure signaled regulatory systems to alter photosystem content (Durnford and Falkowski, 1997; Fujita, 1997), leading to a depressurization of both photosystems and a return to balance between them (Fig. 5). This feedback worked to tune the redox state, or openness, of the photosystems to a relatively narrow and presumably optimal range despite the large changes in illumination and electron production by PSII (Rosenqvist, 2001; Pfannschmidt, 2003).

In the light-limited preshift conditions, reductant produced from net O_2 evolution by photosynthesis was efficiently invested into balanced cell growth in

both high- and low-Ci cells, but after the light increase, half or more of the measured reductant was not accounted for by balanced cell growth. The low growth rate in low-Ci cells may be explained by the reduction of material for building intracellular pools during acclimation at the expense of population growth, including increased Rubisco, maintained PSII and possibly a greater pool of CCM components to better serve the increased photosynthetic rate with more Ci. Electrons generated by photosynthesis can also flow to fates other than reduction of carbon, nitrogen, and sulfur for generation of new organic material. These electrons are also diverted into saturation reactions in existing fatty acids, pyruvate decarboxylation, Glu synthesis, enzyme regulation through reduced thioredoxin (Chitnis, 1996), or to fates outside the cell. Otero and Vincenzini (2004) have shown that excretion of organic material outside the cell was a significant sink for reductant in *Nostoc* and was dependent upon external Ci concentration.

Timescales of Acclimation and the High-Ci Growth Burst

The observed acclimatory changes in pigments, redox balance of the photosystems, and investment of reductant in growth in high- and low-Ci cells occurred at similar rates when expressed on a scale of generational (i.e. relative to growth rate) rather than chronological time. Thus, if arguing relative to the growth of the population, the cells acclimated to the change in light at a similar rate. Indeed, high- and low-Ci cells grown continuously under HL and fully acclimated to it achieved remarkably similar growth rates, photosystem excitation balance, and reductant investment into balanced population growth. Thus, given enough chronological time, high- and low-Ci cells can acclimate comparably to wide shifts in light intensity, albeit through distinct mechanisms. Nevertheless, chronological time constrains achieved acclimation regardless of the generational time spent acclimating to new conditions. HL conditions necessarily last less time than the daylength, and only those cells able to chronologically rapidly exploit new light levels will gain growth benefits of transiently increased light.

During acclimation to HL in the high-Ci cells, growth rate was transiently substantially higher than in cells finally acclimated to the continuous HL condition. This growth burst led to a much larger population of cells in the limited natural time available, which could allow resource sequestration or shading of competing phytoplankton species. Conversely, the growth burst in high-Ci cells was sustained long enough to cover any naturally likely period of increased light. Concurrent with the rise in growth rate in the high-Ci cells was a larger drop in photosystem content and pigmentation than in the low-Ci cells and a smaller rise in Rubisco than in the low-Ci cells. These changes occur in the context of a higher electron transport per photosystem in the high-Ci cells compared to the low-Ci cells, suggesting less investment of photosynthetic reductant needed to be made into the photosynthetic apparatus of the high-Ci cells. High-Ci cells shifted to HL could thus initially invest more photosynthetic reductant in cell growth, supporting the observed growth burst. Once macromolecular complexes of the photosynthetic system declined to levels appropriate to the new light regime, investment may have been withdrawn from accelerated cell growth and returned to balanced pigment and photosystem production, which may explain the slower long-term growth rate in high-Ci cells grown continuously in HL. *S. elongatus* is a model for researching circadian phenomena in cyanobacteria, and investment into the photosynthetic apparatus is modulated with a circadian rhythm when exposed to a light-dark cycle (Suzuki and Johnson, 2001). The observed growth burst in the high-Ci cells may involve entrainment into circadian rhythm in these cells, which would allow the population to benefit from a rapid exploitation of limited-duration HL.

Light acclimation strategies in *S. elongatus* are strongly dependent upon the external Ci concentration. In nature, Ci concentration in freshwater habitats varies from less than our low-Ci level to greater than our high-Ci level, and fluctuates greatly through the year (Cole et al., 1994). Cyanobacteria, especially freshwater β-cyanobacteria, such as *S. elongatus*, which have evolved in an environment with fluctuating Ci (Raven, 2003), have developed diverse CCMs that allow them to sustain similar growth and photosynthetic rates regardless of external Ci, at least under steady illumination and mineral nutrient repletion. Low-Ci cells have an important advantage with their induced CCMs of maintaining photosynthetic competence at far below the minimum Ci tolerable by high-Ci cells. This ability to thrive in low-Ci conditions, however, occurs at the ecologically significant expense of slower acclimation and growth exploitation of increased light.

MATERIALS AND METHODS

Culture Conditions and Light Shift Experiments

Cultures of *Synechococcus elongatus* were separated into distinct metabolic populations of high-Ci status growing in media [Ci] of about 4 mM, achieved through bubbling with 5% CO_2-enriched air at about 40 mL min^{-1}, or low-Ci status growing in media [Ci] of about 0.02 mM, achieved through bubbling with unadulterated air at about 370 μmol CO_2 mol^{-1} at about 200 mL min^{-1}. The growing medium was BG-11 (Rippka et al., 1979), buffered with 10 mM MOPS to achieve stable pH 7.15 in high-Ci media and pH 7.33 in low-Ci media. Ci concentration was stable when measured in cultures growing at both 50 μmol m^{-2} s^{-1} and 500 μmol m^{-2} s^{-1} light. Under these pH conditions, the dominant form of Ci would be bicarbonate, but in the high-Ci media, the concentration of CO_2 would likely be sufficient to fully supply photosynthesis in the high-Ci cells, while in the low-Ci media, the high-affinity inducible bicarbonate and CO_2 transporters would provide the necessary carbon to photosynthesis regardless of external pH or the available form of Ci (Shibata et al., 2002; Badger and Price, 2003). Culture Ci concentrations were directly measured in samples withdrawn from cultures into an air-free syringe, then injected into an inline vial containing citric acid continuously purged with N_2 gas. The acidified and vortexed medium sample quickly (about 1 min)

degassed, with the resulting CO_2 bolus carried through a desiccant cartridge and then into an infrared CO_2 gas analyzer (Qubit Systems, Kingston, Canada). We determined the area under the CO_2 peak from the digitized data trace and compared it to a standard curve made from comparably treated freshly mixed known $NaHCO_3$ solutions.

The high- and low-Ci cultures were grown at 35°C, under 50 μmol photons m^{-2} s^{-1} fluorescent light. These populations were maintained axenically for days to weeks (many tens of generations), continually reinoculated from late log-phase growth into fresh BG-11 medium to keep them in rapid growth at the above conditions. Culture lines were restarted approximately monthly, from axenic cultures maintained on agar plates.

Experimental cultures from each high- and low-Ci population were separately inoculated into polycarbonate tissue culture flasks at approximately 0.2 μg Chl *a* mL^{-1} and grown under continuous light at 50 μmol photons m^{-2} s^{-1} in a controlled environment chamber (Conviron, Winnipeg, Canada) on an orbital shaking table. Experimental cultures were approximately 120 mL volume, 1 cm deep, and continuously and rapidly mixed in the flasks to minimize light gradients and differential shading of the cells. Gas, either 5% CO_2 or ambient air, was supplied via syringe needles extending through a rubber septum sealing the flasks so that the gas was bubbled directly into the medium. Gas was vented from the overlying airspace through a second syringe needle in the rubber septum.

Experimental cultures were grown through approximately three generations to about 1.5 μg Chl *a* mL^{-1} at 50 μmol photons m^{-2} s^{-1} (LL), and then were exposed to 500 μmol photons m^{-2} s^{-1} (HL). This HL level is near the upper end of their tolerable range and has been previously used for studying HL acclimation in this cyanobacterium (Schaefer and Golden, 1989; Clarke et al., 1992; Kulkarni et al., 1992). We measured population growth rates, cell pigmentation, photosynthetic physiology, and macromolecular stoichiometry at several points before and up to 6 h after the shift to HL. We followed these factors for the initial 6 h after the light shift to study the rate and amplitude of acclimation in response to a change of intensity, over a duration appropriate for the habitat of *S. elongatus*.

Growth and Pigmentation

Several times before and then intensively for the 6 h after the light shift, samples of approximately 1 mL volume were removed via sterile syringes pierced through the rubber septum sealing the flask. Whole-cell spectra were measured with a Spectronic Unicam spectrophotometer (VWR Canlab, Mississauga, Canada) to calculate population growth rate and per-cell concentrations of phycocyanin and Chl *a*. We modified the Myers et al. (1980) equations to determine Chl and phycocyanin concentrations by subtracting a wavelength-dependent cell-scattering baseline, rather than only subtracting A_{750}, to give pigment values closer to those determined from solvent extractions. From the pigment absorbance peaks at 630 and 680 nm, we subtracted a logarithmic baseline fit to the whole-cell absorbance values at 535 and 750 nm through 800 nm, at which there is negligible pigment absorbance, and optical density is instead dominated by cell scattering. We empirically related cell population to light scattering at 750 nm to determine spectrophotometer-specific formulae for quantifying cells counted by direct microscopic examination: cells $mL^{-1} = 2.58 \pm 0.06 \times 10^8 A_{750}$ for high-Ci cells and cells $mL^{-1} = 3.70 \pm 0.26 \times 10^8 A_{750}$ for low-Ci cells. These A_{750} calibrations were made for cells growing at 50 μmol photons m^{-2} s^{-1}. Cells grown for many generations at HL (500 μmol photons m^{-2} s^{-1}) show a slightly increased number of cells per A_{750}, yet proportionately they retain the same large difference between high- and low-Ci cells. The small light-related change would have a negligible impact on growth rates (Fig. 2), as we calculated these over discrete time intervals too short to allow any significant change in cells per A_{750}.

Photosynthesis Measurement Apparatus and Simultaneous Light Response Curves

Oxygen evolution, Chl fluorescence, and P700 absorbance changes were measured simultaneously in subsamples taken from the experimental cultures. The 1.65-mL subsamples were suspended in a temperature-controlled quartz cuvette, with fiber-optic light guides to conduct actinic light, saturation light pulses, and probe light for Chl fluorescence and differential absorbance measurements of P700 oxidation. The subsamples were capped with a Clarke-type oxygen electrode modified to seal the sample from the air (YSI, Yellow Springs, OH) and stirred from below with a micromagnetic stirrer. The signals from the oxygen electrode were amplified by a Hansatech control box (King's Lynn, UK). A Walz XE-PAM modulated fluorometer was used to monitor Chl fluorescence and a XE-ST single turnover xenon discharge lamp (Walz, Effeltrich, Germany) was used for measurement of PSII functional absorption cross-sections. A PAM-101 Chl fluorometer modified with the P700DW dual-wavelength differential absorbance probe (Walz) was used to measure the oxidation state of P700, the reaction center of PSI (Klughammer and Schreiber, 1994). White actinic light was supplied by the XE-PAM ranging between 0 and 550 μmol photons m^{-2} s^{-1} by a filtered halogen bulb (transmission <695 nm). This actinic lamp had a spectral emission rich in red light relative to the white fluorescent growth light; thus, under limiting light, our O_2 evolution quantum yield may have overestimated the condition in the growing culture. The majority of our results, however, focus on the light-saturated performance of photosynthesis, where slight differences in the amount of PUR per measured light between different light sources are made irrelevant (Markager and Vincent, 2001). White-light saturation pulses were supplied by an external 300-W halogen bulb filtered (transmission <695 nm) and focused through a Minolta (Missisauga, Canada) camera shutter to provide fast, square, and consistent light profiles at 9,000 μmol photons m^{-2} s^{-1} for 0.5 s (see Fig. 1; e.g. fluorescence and P700 oxidation traces).

Signals generated from the oxygen content of the sample, Chl fluorescence, absorbance changes from P700, and the light level in the cuvette were simultaneously digitized at 20 Hz by a LabPro data logger (Vernier Software, Portland, OR) and displayed real time through a computer interface. These data were subsequently summarized into relevant Chl fluorescence and P700 oxidation parameters by custom-designed software (written by T.D.B. Mac Kenzie). The performance of the automated data summarizing was verified by manually summarizing a subset of the collected data.

Light response curve plots of photosynthetic performance as a function of light intensity (Henley, 1993; Falkowski and Raven, 1997) were used to quantify oxygen evolution from photosynthesis, Chl fluorescence levels, and P700 oxidation states to examine photosystem function. We fit our net O_2 evolution data to the model equation:

$$P = P_{\max}(1 - e^{(-\alpha E/P_{\max})}) - R \quad (1)$$

after Falkowski and Raven (1997), where P is the Chl-specific rate of O_2 evolution (μmol O_2 μmol Chl^{-1} s^{-1}), $P_{\max}$ is the maximum rate of light-saturated O_2 evolution (μmol O_2 μmol Chl^{-1} s^{-1}), α is the initial slope of the light response curve under limiting light (μmol O_2 μmol photons m^2 μmol Chl^{-1}), E is the light intensity (μmol photons m^{-2} s^{-1}), and R is the respiration rate (μmol O_2 μmol Chl^{-1} s^{-1}).

Light response curves can be divided into two sections, a light-limited region in which the photosynthetic rate rises steeply and nearly proportionately with increasing light, α, and a light-saturated range in which the photosynthetic rate reaches a maximum, $P_{\max}$, and no longer increases with increased light. The light-limited range is determined primarily by the capacity for light absorption by the photosynthetic apparatus, while the light-saturated rate is determined by the capacity of the organism to use the reductant and energy derived from photosynthesis, mostly in the fixation of CO_2 (Sukenik et al., 1987; MacIntyre et al., 2002). The light intensity at the transition between the light-limited and light-saturated regions of the light response curve is termed E_k and is determined by:

$$E_k = \frac{P_{\max}}{\alpha}. \quad (2)$$

E_k is considered the optimum light intensity for photosynthesis along the light response curve (Falkowski and Raven, 1997), and so light acclimation is predicted to proceed toward a metabolic condition where E_k approximates the growth light level.

We determined τ^{-1}, which describes the maximum turnover rate (here expressed in electrons s^{-1}) of the PSII pool (Falkowski and Raven, 1997) and is calculated:

$$\tau^{-1} = E_k \sigma_{II} \left(\frac{4 \text{ electrons}}{O_2} \right). \quad (3)$$

We measured the time required for electrons from PSII to reach PSI and begin reducing the P700 pool, t_{red}, after the application of a fast-rising and intense saturation light pulse (Fig. 1). Changes in the speed of electron transfer from PSII to PSI indicate changes in the effective size of the intersystem electron transport chain relative to photosystem content.

We also used light response curves to study the functions of PSII and PSI individually. We measured the proportion of open photosystems, those

available for photochemistry, in the PSII and PSI pools across a range of light intensities simultaneously with the O_2 evolution measurements. We used the established q_P parameter calculated from Chl fluorescence (van Kooten and Snel, 1990) to determine the redox state or approximate fraction of open PSII centers, as:

$$\mathrm{PSII_{open}} = q_P = \frac{F'_m - F_s}{F'_m - F'_o}, \quad (4)$$

where F'_m is the maximum fluorescence elicited by a brief saturating pulse of light, F_s is the steady-state fluorescence level, and F'_o is the minimum level measured on a brief exposure to darkness following actinic illumination (Krause and Weiss, 1991).

We used a parameter analogous to the PSII fluorescence parameter q_P for analyzing the redox state of PSI, based upon P700 oxidation states during steady-state illumination and in response to a saturating light. On exposure to a saturation pulse of intense and fast-rising white light (9,000 μmol m^{-2} s^{-1}; half-rise about 2 ms; $\lambda < 695$ nm), the pool of P700 quickly oxidizes, in 5 to 10 ms, to a plateau level, which is stable for 20 to 50 ms and then reduced by a flood of electrons from PSII (Fig. 1). During actinic illumination, this initial oxidation spike is invariably slightly lower than the maximum oxidation attainable from P700 in the dark with a saturation pulse or with far-red light. The decreased response amplitude under actinic illumination likely occurs from downstream limitation by electron accumulation in a fraction of the initial acceptor pool, A^-, that preempts the flash-induced photooxidation of a proportion of PSI centers (Klughammer and Schrieber, 1994). Under actinic illumination, the steady-state oxidation level of P700 is somewhat elevated, analogous to the F_s fluorescence level measured under illumination in PSII. Thus, by analogy to the PSII q_P parameter, we interpret the proportion of open PSI centers as:

$$\mathrm{PSI_{open}} = \frac{\mathrm{P700_{ox}} - \mathrm{P700_s}}{\mathrm{P700_{ox}} - \mathrm{P700_{red}}}, \quad (5)$$

where $P700_{ox}$ is the absorbance reading when the P700 pool is transiently oxidized by the bright flash superimposed on the background actinic illumination, $P700_s$ is the steady-state oxidation reading during actinic illumination, and $P700_{red}$ is the reading when the P700 pool is fully reduced on brief exposure to darkness. Bukhov and Carpentier (2003) have recently demonstrated that the proportion of reduced (open) PSI centers, like the proportion of open PSII centers, is directly related to the photosystem's photochemical potential, and, thus, we interpret changes in PSI_{open} similarly to $PSII_{open}$.

Photosystem Pool Sizes and Functional Absorption Cross-Sections

In vivo PSII functional, or photochemically active, absorption cross-sections were estimated using pump and probe fluorometry. Chl fluorescence yield of PSII was measured before, and 100 μs after, exposure to microsecond-length light pulses with a dose of approximately 0.1 to 10 photons nm^{-2}. Fluorescence yields were fit to the one-hit Poisson model of Mauzerall and Greenbaum (1989):

$$\Delta\phi_E = \phi_m(1 - e^{(-E\sigma_{II})}), \quad (6)$$

where $\Delta\phi_E$ is fluorescence yield induced over the background level by a light dose of E photons nm^{-2}, ϕ_m is the maximum inducible fluorescence yield over the background level, and σ_{II} is the functional absorption cross-section of PSII in nm^2.

In vivo PSI functional absorption cross-sections were estimated by measuring the rapid (<10 ms) P700 oxidation kinetics during exposure to the fast-rising saturating light (Fig. 1). A second LabPro data logger and computer were used for digitizing P700 oxidation changes at 10,000 Hz, and the level of P700 oxidation at each point during the profile was compared to the accumulated photon dose applied from the 9,000 μmol photons m^{-2} s^{-1} white-light saturation pulse. Total light exposure during the rising profile of P700 oxidation ranged up to approximately 25 photons nm^{-2}, comparable to the range of quantum dose for the PSII cross-section measurements. Like the fluorescence response of PSII, the P700 oxidation response was fit to quantum dose by the Poisson model, and the resultant functional absorption cross-section was denoted σ_I. This approach gave reasonable estimates of a functional absorption cross-section of PSI, although a potential confounding factor is that the measurements extended over a time interval where rereduction of P700 could occur, potentially resulting in an underestimate of the functional absorption cross-section. Manodori and Melis (1984) used a similar approach to measure changes in excitation potential of PSI in *Anacystis nidulans* grown in different light environments. Murakami and Fujita (1991b) detailed the time constants for reduction of P700 in a similar cyanobacterium, *Synechocystis* PCC6714, with a relatively high PSI-to-PSII ratio like our cells. Oxidized P700 centers are initially rereduced by a small pool of electron carriers local to PSI with a half-life of up to 0.4 ms. The bulk of reductant, however, arrives with half-lives of about 10 to 15 ms and 20 ms from reductant migrating through the Cyt B6-f complex from the plastoquinone pool. In our oxidation traces we see a similar window between about 0.5 and 10 ms, before the arrival of the main reductant flux, where P700 oxidation rises smoothly with light dose (Fig. 1) in a form well explained by the Poisson model (Mauzerall and Greenbaum, 1989).

We estimated the numbers of photosystems in the cells using σ_{II}, Chl *a*, and the light-limited slope of oxygen evolution (α), modified from Falkowski and Raven (1997) to give PSII $cell^{-1}$:

$$\mathrm{PSII\ cell^{-1}} = \frac{\alpha(\mathrm{Chl}\ a\ \mathrm{cell^{-1}})}{\sigma_{II}} \quad (7)$$

and PSI numbers as

$$\mathrm{PSI\ cell^{-1}} = \frac{(\mathrm{Chl}\ a - 36\ \mathrm{Chl}\ a\ \mathrm{PSII^{-1}})}{96\ \mathrm{Chl}\ a\ \mathrm{PSI^{-1}}}. \quad (8)$$

Photosystem Chl molecules were taken as 36 per PSII monomer (Ferreira et al., 2004) and 96 per PSI monomer (Chitnis, 2001). This functional determination of photosystem numbers is more appropriate for our purpose than a direct gross quantitation such as immunodetection, which cannot distinguish between functioning and nonfunctioning PSII centers, or subpopulations of photosystems with differing relations to their light-absorbing antennae or local electron transport system (Walters and Horton, 1993; Prasil et al., 1996). This functional quantitation of photosystems, particularly PSII, encompasses their number, function, and heterogeneity into a functional sum in terms of electron transport performance.

Rubisco Quantitation

Catalytic sites of the enzyme Rubisco were quantified in subsamples taken from the batch cultures simultaneously with those used for physiological measurements. Rubisco is the enzyme that catalyzes the carboxylation reaction that fixes CO_2 into organic carbon in the reductant-consuming Calvin cycle. Here, we use Rubisco concentration as an indicator of carbon fixation and reductant sink potential.

We centrifuged 1-mL aliquots of medium (containing between 1.5 and 3 μg Chl) at 12,000*g* for 5 min immediately after withdrawal from the culture and stored the cell pellets at about −20°C until extraction. The protein extraction occurred in 200 μL of solubilization buffer (140 mM Tris base, 105 mM Tris-HCl, 0.5 mM EDTA, 2% LDS, 10% glycerol), which was frozen in liquid nitrogen, then thawed while sonicating with a Branson Ultrasonics (Danbury, CT) model 450 sonicator for 50 s in two cycles. Dithiothreitol was added to the solubilization buffer (final concentration 50 mM), and the samples were incubated at 65°C for 5 min to denature and solubilize the proteins. The protein samples were centrifuged at 12,000*g* for 2 min to pellet insoluble cell debris, then frozen and stored at approximately −20°C until use.

The protein samples were separated on precast 10% linear BisTris polyacrylamide NuPage gels (Invitrogen, Carlsbad, CA) in an XCell electrophoresis system (Invitrogen). The samples were loaded on an equal-cell-number basis (2.3×10^6 cells per lane; approximately 50–80 pmol Chl *a* per lane), then run at 200 V for 1 h in 1× MES buffer (Invitrogen). At least two lanes per gel were loaded with spinach Rubisco (AgriSera, Vännäs, Sweden) as a quantitative standard. The separated proteins were transferred onto PVDF membrane (Bio-Rad Laboratories, Hercules, CA) with 1× NuPage transfer buffer in the XCell (Invitrogen) at 30 V for 1 h. The membrane was immediately placed in a 2% ECL Advance blocking buffer (Amersham-Pharmacia Biotech, Uppsala) in Tris-buffered saline (TBS-T: 20 mM Tris base, 500 mM NaCl, 0.1% Tween 20, pH 7.6) for 1 h at room temperature. The membrane was then incubated with a Global anti-RbcL (large subunit of Rubisco) antibody raised in chicken (AgriSera) at a dilution of 1:50,000 in 10 mL of 2% blocking buffer for 1 h at room temperature. This antibody is directed against a region of the RbcL protein identical in sequence in *S. elongatus* and from spinach. The membrane was exhaustively rinsed in TBS-T and then incubated with a HRP-conjugated

antichicken secondary antibody raised in goat (Abcam Scientific, Cambridge, UK) at a dilution of 1:50,000 in 10 mL of blocking buffer for 1 h at room temperature. Again, the membrane was exhaustively rinsed in TBS-T and then detected with ECL Advance chemiluminescent development reagents (Amersham-Pharmacia Biotech) according to the manufacturer's protocol. The chemiluminescent blots were imaged with a Fluor-S Max camera system (Bio-Rad) and signals were quantified using Quantity One software (Bio-Rad).

Growth Investment of Biosynthetic Electron Transport

We calculated the reductant required for the balanced growth of cells in the high- and low-Ci cells as a function of the reductant produced by the cells.

$$\frac{\text{Growth}}{\text{Reductant}} = \frac{(2^{(86{,}400\times\mu_E)^{-1}} - 1)(\text{C}\times\text{cell}^{-1})(5.919\text{e}^{-}\times\text{C}^{-1})}{\text{P}_\text{E}(4\text{e}^{-}\times\text{O}_2^{-1})} \quad (9)$$

The exponential function in Equation 9 calculates the growth rate (μ_E) at a specific light level (E) as the change in cell number, $\text{cell}^{-1}\ \text{s}^{-1}$, multiplied by the empirically estimated carbon content per cell, to compare to oxygen produced by photosynthesis at that light (P_E), converted to equivalent electrons s^{-1}. The number of carbon atoms per cell, 3.26×10^{10} for high-Ci cells and 2.27×10^{10} for low-Ci cells, was estimated by quantifying CO_2 produced after combustion of cell samples. The cell samples were rinsed with distilled water and dried at about 70°C under dry N_2 gas in glass ampules. The ampules were sealed, containing excess O_2, then combusted at 500°C overnight. CO_2 resulting from the sample combustion was quantified with an infrared CO_2 gas analyzer (Qubit Systems) using standards of 100 mmol Gly solution (Sigma, St. Louis), dried and combusted in the same manner as the cell samples. The 5.919 electrons per carbon reduced were estimated as the sum of the electrons required to reduce carbon, nitrogen, and sulfur in the ratio of their estimated abundance in the cells. Electrons required to reduce carbon alone were estimated based on the reactions $CO_2+4e^-\rightarrow[CH_2O]$ to produce C^0 for carbohydrate-C and most protein-C, and $CO_2+6e^-\rightarrow[CH_2]$ to produce C^{2-} for lipid-C. We assumed an 84:16 C^0:C^{2-} ratio from literature values of lipid content (Lourenco et al., 2002) to arrive at 4.320 e^- per average C atom. The electrons per nitrogen reduced were based on the reaction $NO_3^-+8e^-\rightarrow NH_4^+$ as well as two additional electrons required for the reductive amination reaction to assimilate the ammonium into amino acids. The only nitrogen source in the medium was nitrate; *S. elongatus* does not fix nitrogen, the amount of nitrogen required was based upon the average N content of four *Synechococcus* strains, 0.146 N per C (Bertilsson et al., 2003; Heldal et al., 2003), to give 1.552 e^- required for nitrogen per carbon assimilated. Similarly, we accounted for sulfur reduction (from sulfate) based on the reaction $SO_4^{3-}+7e^-\rightarrow SH^-$ and an estimated S content of the cells of 0.0066 S per C (Heldal et al., 2003; Ho et al., 2003) to give 0.046 e^- required for sulfur per carbon assimilated. Other elements required for growth were not accounted for, as most other high-concentration constituents, such as hydrogen, oxygen, phosphate, magnesium, and calcium, are not reduced during assimilation, and all other cell constituents were quantitatively negligible.

ACKNOWLEDGMENTS

We thank AgriSera for supplying the Global anti-RbcL antibody and Dr. Amanda Cockshutt and Mr. Chris Brown for optimizing the protein immunodetection protocols.

Received June 15, 2004; returned for revision July 29, 2004; accepted August 2, 2004.

LITERATURE CITED

Allen J (2003) Cyclic, pseudocyclic and noncyclic photophosphorylation: new links in the chain. Trends Plant Sci **8:** 15–19

Anderson J, Park Y-I, Chow WS (1998) Unifying model for the photoinactivation of Photosystem II *in vivo* under steady-state photosynthesis. Photosynth Res **56:** 1–13

Badger MR, Price GD (2003) CO_2 concentrating mechanisms in cyanobacteria: molecular components, their diversity and evolution. J Exp Bot **54:** 609–622

Behrenfeld M-J, Prasil O, Kolber ZS, Babin M, Falkowski PG (1998) Compensatory changes in Photosystem II electron turnover rates protect photosynthesis from photoinhibition. Photosynth Res **58:** 259–268

Bertilsson S, Berglund O, Karl DM, Chisholm SW (2003) Elemental composition of marine *Prochlorococcus* and *Synechococcus*: implications for the ecological stoichiometry of the sea. Limnol Oceanogr **48:** 1721–1731

Bukhov NG, Carpentier R (2003) Measurement of photochemical quenching of absorbed quanta in photosystem I of intact leaves using simultaneous measurements of absorbance changes at 830 nm and thermal dissipation. Planta **216:** 630–638

Campbell D, Hurry VM, Clarke AK, Gustafsson P, Öquist G (1998) Chlorophyll fluorescence analysis of cyanobacterial photosynthesis and acclimation. Microbiol Mol Biol Rev **62:** 667–683

Clarke AK, Soitamo A, Gustafsson P, Öquist G (1992) Rapid interchange between two distinct forms of cyanobacterial photosystem II reaction-center protein D1 in response to photoinhibition. Proc Natl Acad Sci USA **90:** 9973–9977

Chitnis PR (1996) Photosystem I. Plant Physiol **111:** 661–669

Chitnis PR (2001) Photosystem I: function and physiology. Annu Rev Plant Physiol Plant Mol Biol **52:** 593–626

Cole JJ, Caraco NF, Kling GW, Kratz TK (1994) Carbon dioxide supersaturation in the surface waters of lakes. Science **265:** 1568–1570

Durnford DG, Falkowski PG (1997) Chloroplast redox regulation of nuclear gene transcription during photoacclimation. Photosynth Res **53:** 229–241

Eley J (1980) Effect of carbon dioxide concentration on pigmentation in the blue-green alga *Anacystis nidulans*. Plant Cell Physiol **12:** 311–316

Escoubas JM, Lomas M, Laroche J, Falkowski PG (1995) Light intensity regulation of *cab* gene transcription is signaled by the redox state of the plastoquinone pool. Proc Natl Acad Sci USA **92:** 10237–10241

Falkowski P, Raven JA (1997) Aquatic Photosynthesis. Blackwell, Oxford

Ferreira KN, Iverson TM, Maghlaoui K, Barber J, Iwata S (2004) Architecture of the photosynthetic oxygen-evolving center. Science **303:** 1831–1838

Fujita Y (1997) A study on the dynamic features of photosystem stoichiometry: accomplishments and problems for future studies. Photosynth Res **53:** 83–93

Fujita Y, Murakami A, Ohki K (1987) Regulation of photosystem composition in the cyanobacterial photosynthetic system: the regulation occurs in the response to the redox state of the electron pool located between the two photosystems. Plant Cell Physiol **28:** 283–292

Heldal M, Scanlan DJ, Norland S, Thingstad F, Mann NH (2003) Elemental composition of single cells of various strains of marine *Prochlorococcus* and *Synechococcus* using X-ray microanalysis. Limnol Oceanogr **48:** 1732–1743

Henley WJ (1993) Measurement and interpretation of photosynthetic light-response curves in algae in the context of photoinhibition and diel changes. J Phycol **29:** 729–739

Herbert SK, Martin RE, Fork DC (1995) Light adaptation of cyclic electron transport through photosystem I in the cyanobacterium *Synechococcus* sp. PCC 7942. Photosynth Res **46:** 277–285

Ho TY, Quigg A, Finkel ZV, Milligan AJ, Wyman K, Falkowski PG, Morel FMM (2003) The elemental composition of some marine phytoplankton. J Phycol **39:** 1145–1159

Huner NPA, Maxwell DP, Gray GR, Savitch LV, Laudenbach DE, Falk S (1995) Photosynthetic response to light and temperature: PSII excitation pressure and redox signalling. Acta Physiol Plant **17:** 167–176

Huner NPA, Öquist G, Sarhan F (1998) Energy balance and acclimation to light and cold. Trends Plant Sci **3:** 224–230

Kana TM, Geider RJ, Critchley C (1997) Regulation of photosynthetic pigments in micro-algae by multiple environmental factors: a dynamic balance hypothesis photoacclimation. New Phytol **137:** 629–638

Kana R, Lazár D, Prásil O, Naus J (2002) Experimental and theoretical studies on the excess capacity of Photosystem II. Photosynth Res **72:** 271–284

Kaplan A, Helman Y, Tchernov D, Reinhold L (2001) Acclimation of photosynthetic microorganisms to changing ambient CO_2 concentrations. Proc Natl Acad Sci USA **98:** 4817–4818

Klughammer C, Schreiber U (1994) An improved method, using saturating light pulses, for the determination of photosystem I quantum yield via $P700^+$-absorbance changes at 830 nm. Planta **192:** 261–268

Krause GH, Weiss E (1991) Chlorophyll fluorescence and photosynthesis: the basics. Annu Rev Plant Physiol Plant Mol Biol **42:** 313–349

Kulkarni RD, Schaefer MR, Golden SS (1992) Transcriptional and post-

transcriptional components of *psbA* response to high light intensity in *Synechococcus* sp. strain PCC 7942. J Bacteriol **174:** 3775–3781

Li Q, Canvin DT (1997) Oxygen photoreduction and its effect on CO_2 accumulation and assimilation in air-grown cells of Syn*echococcus* UTEX 625. Can J Bot **75:** 274–283

Li L-A, Tabita F (1994) Transcription control of ribulose bisphosphate carboxylase/oxygenase activase and adjacent genes in *Anabaena* species. J Bacteriol **176:** 6697–6706

Lourenco SO, Barbarino E, Mancini-Filho J, Schinke KP, Aidar E (2002) Effects of different nitrogen sources on the growth and biochemical profile of 10 marine microalgae in batch culture: an evaluation for aquaculture. Phycologia **41:** 158–168

MacIntyre HL, Kana TM, Anning T, Geider RJ (2002) Photoacclimation of photosynthesis irradiance response curves and photosynthetic pigments in microalgae and cyanobacteria. J Phycol **38:** 17–38

Manodori A, Melis A (1984) Photochemical apparatus organisation in *Anacystis nidulans* (Cyanophyceae). Plant Physiol **74:** 67–71

Markager S, Vincent W (2001) Light absorption by phytoplankton: development of a matching parameter for algal photosynthesis under different spectral regimes. J Plankton Res **23:** 1373–1384

Mauzerall D, Greenbaum NL (1989) The absolute size of a photosynthetic unit. Biochim Biophys Acta **974:** 119–140

McGinn PJ, Price GD, Badger MR (2004) High light enhances the expression of low-CO_2-inducible transcripts involved in the CO_2-concentrating mechanism in *Synechocystis* sp. PCC6803. Plant Cell Environ **27:** 615–626

Melis A, Brown JS (1980) Stoichiometry of system I and system II reaction centers and of plastoquinone in different photosynthetic membranes. Proc Natl Acad Sci USA **77:** 4712–4716

Miskiewicz E, Ivanov AG, Huner NPA (2002) Stoichiometry of the photosynthetic apparatus and phycobilisome structure of the cyanobacterium *Plectonema boryanum* UTEX 485 are regulated by both light and temperature. Plant Physiol **130:** 1414–1425

Müller C, Reuter W, Wehrmeyer W, Dau H, Senger H (1993) Adaptation of the photosynthetic apparatus of *Anacystis nidulans* to irradiance and CO_2-concentration. Bot Acta **106:** 480–487

Murakami A, Fujita Y (1991a) Regulation of photosystem stoichiometry in the photosynthetic system of the cyanophyte *Synechocystis* PCC 6714 in response to light intensity. Plant Cell Physiol **32:** 223–230

Murakami A, Fujita Y (1991b) Steady state of photosynthetic electron transport in cells of the cyanophyte *Synechocystis* PCC 6714 having different stoichiometry between PS I and PS II: analysis of flash-induced oxidation-reduction of cytochrome f and P700 under steady state of photosynthesis. Plant Cell Physiol **32:** 213–222

Murakami A, Kim S-J, Fujita Y (1997) Changes in photosystem stoichiometry in response to environmental conditions for cell growth observed with the cyanophyte *Synechocystis* PCC 6714. Plant Cell Physiol **38:** 392–397

Muramatsu M, Hihara Y (2003) Transcriptional regulation of genes encoding subunits of photosystem I during acclimation to high-light conditions in *Synechocystis* sp. PCC 6803. Planta **216:** 446–453

Myers J, Graham JR, Wang RT (1980) Light harvesting in *Anacystis nidulans* studied in pigment mutants. Plant Physiol **66:** 1144–1149

Ogawa T, Kaplan A (2003) Inorganic carbon acquisition systems in cyanobacteria. Photosynth Res **77:** 105–115

Öquist G, Chow WS, Anderson JM (1992) Photoinhibition of photosynthesis represents a mechanism for long-term regulation of photosystem II. Planta **186:** 450–460

Ort DR, Baker NR (2002) A photoprotective role for O_2 as an alternative electron sink in photosynthesis? Curr Opin Plant Biol **5:** 193–198

Otero A, Vincenzini M (2004) *Nostoc* (Cyanophyceae) goes nude: extracellular polysaccharides serve as a sink for reducing power under unbalanced C/N metabolism. J Phycol **40:** 74–81

Pfannschmidt T (2003) Chloroplast redox signals: how photosynthesis controls its own genes. Trends Plant Sci **8:** 33–41

Prasil O, Kolber Z, Berry J, Falkowski P (1996) Cyclic electron flow around photosystem II in vivo. Photosynth Res **48:** 395–410

Raven JA (2003) Inorganic carbon concentrating mechanisms in relation to the biology of algae. Photosynth Res **77:** 155–171

Rippka R, Deruelles J, Waterbury JB, Herdman M, Stanier RY (1979) Generic assignments, strain histories and properties of pure cultures of cyano-bacteria. J Gen Microbiol **11:** 1–61

Rippka R, Herdman M (1992) Pasteur Culture Collection of Cyanobacterial Strains in Axenic Culture, Catalogue and Taxonomic Handbook. Institut Pasteur, Paris

Rodríguez-Buey ML, Orús MI (2001) The response of *Synechococcus* PCC7942 (Cyanophyta) to changes in CO_2 supply in relation to the acclimation of the CO_2-concentrating mechanism. I: physiological study. J Plant Physiol **158:** 325–334

Rosenqvist E (2001) Light acclimation maintains the redox state of the PS II electron acceptor Q_A within a narrow range over a broad range of light intensities. Photosynth Res **70:** 299–310

Schaefer MR, Golden SS (1989) Light availability influences the ratio of two forms of D1 in cyanobacterial thylakoids. J Biol Chem **264:** 7412–7417

Schubert H, Matthijs H, Mur LR, Schiewer U (1995) Blooming of cyanobacteria in turbulent water with steep light gradients: the effect of intermittent light and dark periods on the oxygen evolution capacity of *Synechocystis* sp. PCC 6803. FEMS Microbiol Ecol **18:** 237–245

Shibata M, Ohkawa H, Katoh H, Shimoyama M, Ogawa T (2002) Two CO_2-uptake systems: four systems for inorganic carbon acquisition in *Synechocystis* sp. strain PCC6803. Funct Plant Biol **29:** 123–129

Smith B, Melis A (1988) Photochemical apparatus organization in the diatom *Cylindrotheca fusiformis*: photosystem stoichiometry and excitation distribution in cells grown under high and low irradiance. Plant Cell Physiol **29:** 761–769

Sonoike K, Hihara Y, Ikeuchi M (2001) Physiological significance of the regulation of photosystem stoichiometry upon high light acclimation of *Synechocystis* sp. PCC6803. Plant Cell Physiol **42:** 379–384

Sukenik A, Bennett J, Falkowski P (1987) Light-saturated photosynthesis—limitation by electron transport or carbon fixation. Biochim Biophys Acta **891:** 205–215

Suzuki L, Johnson CH (2001) Algae know the time of day: circadian and photoperiodic programs. J Phycol **37:** 933–942

van Kooten O, Snel JFH (1990) The use of chlorophyll fluorescence nomenclature in plant stress physiology. Photosynth Res **25:** 147–150

Vasilikiotis C, Melis A (1994) Photosystem II reaction center damage and repair cycle: chloroplast acclimation strategy to irradiance stress. Proc Natl Acad Sci USA **91:** 7222–7226

Vierling E, Alberte R (1980) Functional organization and plasticity of the photosynthetic unit of the cyanobacterium *Anacystis nidulans*. Physiol Plant **50:** 93–98

Walters RG, Horton P (1993) Theoretical assessment of alternative mechanisms for non-photochemical quenching of PS II fluorescence in barley leaves. Photosynth Res **36:** 119–139

Webb M, Melis A (1995) Chloroplast response in *Dunaliella salina* to irradiance stress effect on thylakoid membrane protein assembly and function. Plant Physiol **107:** 885–893

Woodger FJ, Badger MR, Price GD (2003) Inorganic carbon limitation induces transcripts encoding components of the CO_2-concentrating mechanism in *Synechococcus* sp. PCC7942 through a redox-independent pathway. Plant Physiol **133:** 2069–2080